Theoretical Study of the Reaction $^1[:CH_2] + CHO^+ \rightarrow CH_3^+ + CO$

Natalia Díaz and Dimas Suárez

Departamento de Química Física y Analítica, Facultad de Química, Universidad de Oviedo, Julián Clavería, 8, 33006 Oviedo, Spain

Tomás L. Sordo*,†

Department of Chemistry, Hunter College of the City University of New York, 695 Park Avenue, New York, New York 10021

Received: June 4, 1998; In Final Form: August 17, 1998

An ab initio study was performed of the reactions of formyl and isoformyl cations with singlet methylene $^1[:CH_2]$, which plays an important role in the ionic mechanisms for the formation of soot in flames. The corresponding potential energy surface (PES) was studied at the MP2/6-311++G(d,p) level of theory, and single-point calculations on the MP2 geometries were carried out at the CCSD(T)/6-311++G(d,p) and MP2/6-311++G(3df,3pd) levels. According to our results, the interaction of $^1[:CH_2]$ with both HCO^+ and COH^+ cations directly leads to two $C_2H_3O^+$ cyclic intermediates, about 83 and 22 kcal/mol, respectively, more stable than methylene and the formyl cation. A linear CH_2COH^+ structure may also be formed from the interaction between $^1[:CH_2]$ and COH^+ fragments that is 133 kcal/mol more stable than the reactants. Different transition structures for the 1,2-H or 1,2-CH_3^+ shift and/or ring-opening of these intermediates were located, thus allowing us to predict that open-chain structures such as CH_3CO^+ and $CH_3^+\cdots OC$ (∼138 and 85 kcal/mol more stable than reactants, respectively) may dissociate into the $CO + CH_3^+$ products. Proton-transfer mechanisms are also possible for this process through hydrogen-bonded $CH_2-H\cdots CO$ and $CH_2-H\cdots OC$ complexes characterized as minima on the PES. The transition structures for the H-shift corresponding to the isomerization of the CHO^+ moiety from formyl into isoformyl are considerably stabilized by the attachment of $^1[:CH_2]$ to the π CO bond compared with the transition structures for the uncatalyzed process $HCO^+ \rightarrow COH^+$.

Introduction

Many chemical mechanisms have been proposed for the formation of soot in flames.[1,2] Ions may participate in the formation of soot in fuel-rich flames at three stages: nucleation; coagulation of large aromatic ions; coagulation of soot particles. It has been proposed that the ionic mechanism[3−5] may compete with free radical mechanisms especially in two of the stages where charged species may be important: formation of the initial soot precursor species leading to incipient soot; coagulation of small soot particles. In the nucleation steps leading to large molecular species the ionic mechanism may compete with free radical mechanisms because the rate coefficients of ion−molecule reactions are greater than those for free radical reactions, thus compensating for the lower concentrations of ions. The rate of coagulation of large ions or charged particles is enhanced over that of neutral species because of electrostatic effects.

The propargylium ion, $C_3H_3^+$, is the dominant ion in fuel-rich and sooting flames[6−8] and has been proposed as a precursor of soot. It has been demonstrated, in modeling studies[6] of fuel-rich systems, that when the CH radical is electronically excited, the chemiionization reaction

$$CH + O \rightarrow CHO^+ + e^- \quad (1)$$

is responsible for ionization in very rich hydrocarbon flames. Under these conditions an important source of $C_3H_3^+$ has been confirmed to be the following reactions:

$$CH_2 + CHO^+ \rightarrow CH_3^+ + CO \quad (2)$$

$$CH_3^+ + C_2H_2 \rightarrow C_3H_3^+ + H_2 \quad (3)$$

and/or

$$CHO^+ + H_2O \rightarrow CO + H_3O^+ \quad (4)$$

$$H_3O^+ + C_3H_2 \rightarrow C_3H_3^+ + H_2O \quad (5)$$

In the present work, the mechanisms through which the singlet methylene reacts with the CHO^+ cation, eq 2, will be investigated using the ab initio molecular orbital method to characterize the corresponding potential energy surface (PES). A detailed study of the most significant stable structures and transition structures (TSs) connecting them on the PES seems valuable to get a deeper knowledge of the features determining their dynamical behavior.

Methods of Calculation

Ab initio calculations were carried out with the Gaussian 94 series of programs.[9] Stable species were fully optimized and TSs located using Schlegel's algorithm[10] at the MP2/6-311++G(d,p) theory level.[11] All the critical points were further charac-

† On leave from Departamento de Química Física y Analítica, Universidad de Oviedo, Spain.

10.1021/jp982482v CCC: $15.00
Published on Web 11/04/1998

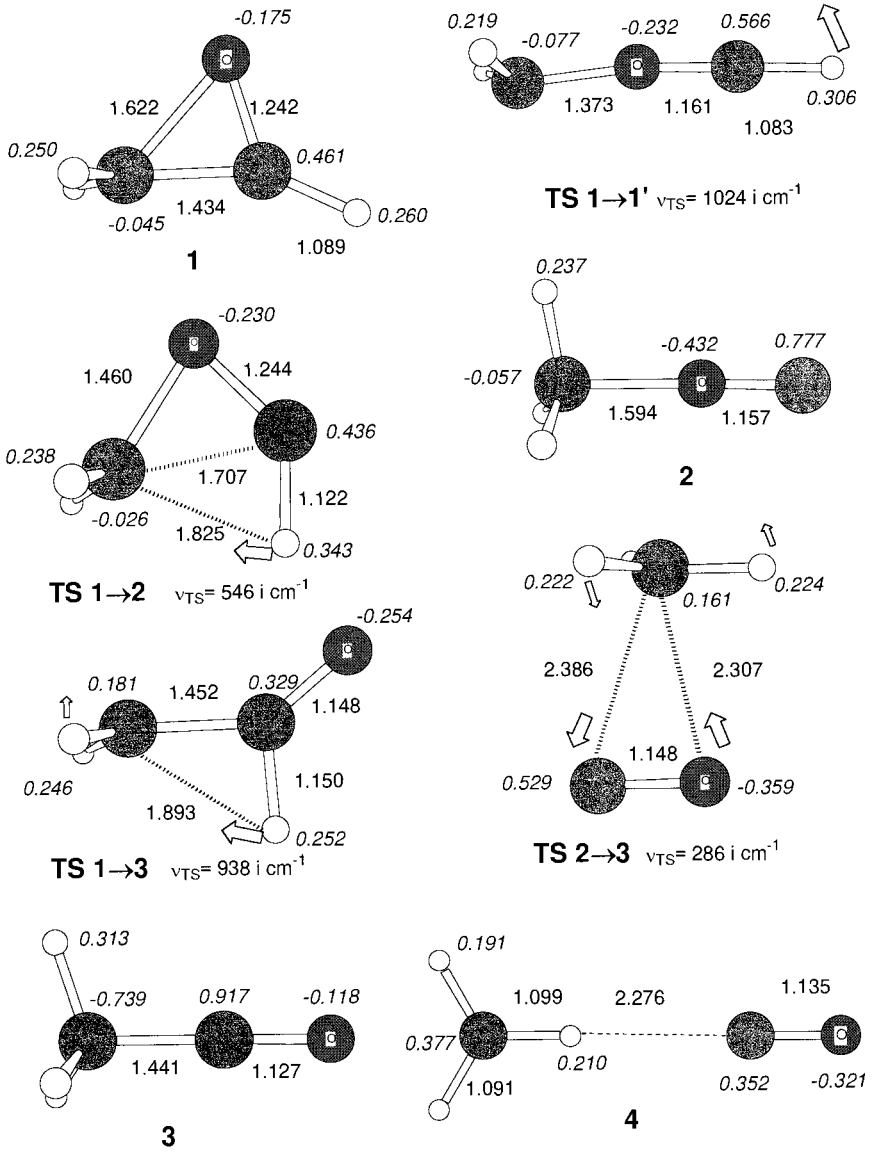

Figure 1. MP2/6-311++G(d,p) optimized geometries of the TSs and intermediates located for the reaction of formyl cation with $^1[:CH_2]$. Bond lengths are given in angstroms. NPA atomic charges are shown in italics. At TSs, hollow arrows sketch the main components of the corresponding transition vectors.

terized, and the zero-point vibrational energy (ZPVE) was evaluated by analytical MP2/6-311++G(d,p) computations of harmonic frequencies. In addition, CCSD(T)/6-311++G(d,p) single-point calculations were carried out on the MP2/6-311++G(d,p) geometries in order to estimate the effect of more elaborated *N*-electron treatments on the calculated relative energies.[12] Similarly, the influence of large basis sets on the relative energies of the MP2/6-311++G(d,p) optimized structures was estimated by means of single-point MP2 calculations using the 6-311++G(3df,3pd) basis set. The frozen core approximation was used in all the calculations.

Thermodynamic data (700 K, 1 bar) were computed to obtain results that can be more readily compared with experimental results within the ideal gas, rigid rotor, and harmonic oscillator approximations.[13]

Reaction paths passing through all the TSs located in this work were studied by MP2/6-311++G(d,p) intrinsic reaction coordinate (IRC) calculations using the Gonzalez and Schlegel method[14] implemented in Gaussian 94. Atomic charges were computed by carrying out a natural population analysis[15] (NPA) on the corresponding MP2/6-311++G(d,p) density matrices for all the structures. In addition, some intermediates were analyzed by means of a population analysis carried out to expand the molecular orbitals (MOs) of a complex system in terms of the MOs of its fragments (using the geometry each fragment has in the corresponding intermediates), thus allowing a more detailed characterization of the electronic interactions between reactants.[16] This analysis was performed using a revised version of the ANACAL program.[17]

Results and Discussion

We will investigate the reaction of both formyl HCO^+ and isoformyl COH^+ cations with singlet methylene $^1[:CH_2]$ to yield the methyl cation and carbon monoxide. Figures 1 and 2 display, respectively, the optimized geometry of the minimum energy structures and the TSs located along the reaction coordinate for both processes. Table 1 presents the corresponding relative energies at the different theory levels employed in this work and the thermodynamic data calculated using the MP2/6-311++G(d,p) analytical frequencies. Figure 3 shows the resultant energy profiles for both processes. Unless otherwise stated, the relative energies given in the text were computed

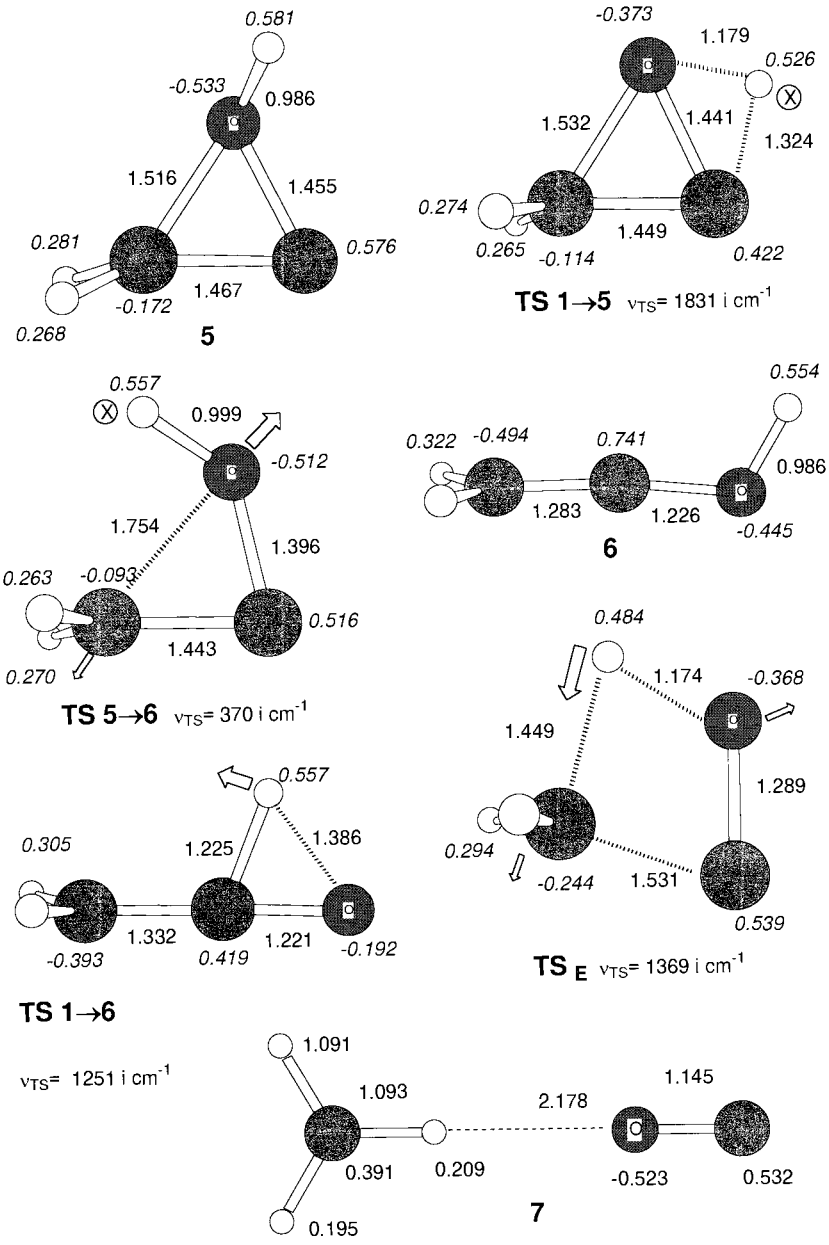

Figure 2. MP2/6-311++G(d,p) optimized geometries of the TSs and intermediates located for the reaction of isoformyl cation with $^1[:CH_2]$. Bond lengths are given in angstroms. NPA atomic charges are shown in italics. At TSs, hollow arrows sketch the main components of the corresponding transition vectors.

using electronic energies approximated in an additive fashion[18] as follows:

$$E[\text{CCSD(T)/6-311++G(3df,3pd)}] \approx E[\text{CCSD(T)/6-311++G(d,p)}] + E[\text{MP2/6-311++G(3df,3pd)}] - E[\text{MP2/6-311++G(d,p)}]$$

and including ZPVE corrections from the MP2/6-311++G(d,p) unscaled frequencies. These electronic energies were also used to evaluate thermodynamic data.

To calibrate the methodology to be used in the determination of the energetics as well as the mechanism of the title reaction, the methylene singlet−triplet energy separation, S−T, was calculated using the corresponding MP2/6-311++G(d,p) geometries for the singlet and triplet $[:CH_2]$. Experimental studies have shown that the triplet is in the ground state with a S−T gap equal to ca. 9 kcal/mol.[19] Our best theoretical estimation is 9.2 kcal/mol, which is in excellent agreement with the experimental value and with theoretical results previously reported.[20]

According to experimental determinations,[21] the formyl cation, HCO^+, is 38.2 kcal/mol more stable than the other isomeric structure, the isoformyl cation COH^+. Our best theoretical calculations give 36.6 kcal/mol for this energy difference, differing in only 1.6 kcal/mol from the experimental value. The 1,2-H-shift TS for the direct isomerization of HCO^+ to COH^+ has a high energy barrier of 72.0 kcal/mol.

To further assess the reliability of the procedure used in this work to evaluate relative energies, the S−T $^1[:CH_2]$ energy and the energy profile for the $HCO^+ \rightarrow COH^+$ process were also calculated at the CCSD(T)/6-311++G(3df,3pd)//MP2/6-311++G(d,p) level including the MP2/6-311++G(d,p) ZPVE correction. The obtained S−T gap is 9.6 kcal/mol, while the corresponding energy barrier and reaction energy for the isomerization are 72.3 and 37.1 kcal/mol, respectively. These

TABLE 1: Relative Energies (kcal/mol) of the Chemically Important Structures Located on the $^1[:CH_2] + CHO^+$ Ion−Molecule Reaction in Gas Phase at the Various Theory Levels Used in This Work[a]

structures	MP2/6-311++ G(d,p)	ZPVE[b]	CCSD(T)/ 6-311++G(d,p)	MP2/6-311++ G(3df,3pd)	ΔH^c	ΔG^c
fragments						
$^1[:CH_2] + HC{=}O^+$	0.0	0.0	0.0	0.0	0.0	0.0
$^3[:CH_2] + HC{=}O^+$	−17.4	0.4	−12.1	−14.9	−8.7	−9.0
$^1[:CH_2] + C{=}OH^+$	47.4	−2.0	40.2	45.8	38.1	36.0
$CO + CH_3^+$	−69.1	2.3	−67.5	−68.1	−66.0	−65.7
$H_2C{=}O + CH^+$	65.6	0.3	58.4	66.8	59.0	59.0
$H_2C{=}C{=}O + H^+$	56.0	−1.1	64.3	50.8	60.3	66.5
intermediates						
CH_2CHO^+ (cyclic), **1**	−90.8	7.7	−86.2	−95.2	−85.4	−59.5
CH_3OC^+ (linear), **2**	−89.1	6.7	−89.1	−91.9	−86.5	−64.8
CH_3CO^+ (linear), **3**	−151.0	7.4	−143.5	−153.3	−140.4	−115.6
$H_2CH{\cdots}CO$ (linear), **4**	−75.6	3.3	−73.4	−75.3	−67.1	−48.3
CH_2COH^+ (cyclic), **5**	−21.6	5.9	−23.8	−26.2	−24.2	0.1
CH_2COH^+ (linear), **6**	−100.6	6.4	−97.9	−105.5	−97.9	−74.0
$H_2CH{\cdots}OC$ (linear), **7**	−72.1	3.0	−71.5	−71.7	−67.5	−49.4
transition structures						
$CHO^+ \rightarrow COH^+$	82.6	−4.2	77.3	81.5	71.2	68.7
$CH_2CHO^+ \rightarrow CH_2CHO^+$, **TS 1→1′**	−10.1	4.7	−8.2	−16.4	3.0	12.6
$CH_2CHO^+ \rightarrow CH_3OC^+$, **TS 1→2**	−27.1	5.0	−26.9	−32.0	−29.7	−6.5
$CH_2CHO^+ \rightarrow CH_3CO^+$, **TS 1→3**	−57.2	4.1	−61.0	−63.4	−64.8	−39.0
$CH_3OC^+ \rightarrow CH_3CO^+$, **TS 2→3**	−73.9	4.3	−72.9	−75.0	−71.0	−51.5
$CH_2CHO^+ \rightarrow CH_2COH^+$, **TS 1→5**	3.3	3.5	4.6	−2.6	−0.2	25.4
$CH_2CHO^+ \rightarrow CH_2COH^+$, **TS 1→6**	−43.5	2.8	−37.3	−48.8	−41.5	−17.4
$CH_2COH^+ \rightarrow CH_2COH^+$, **TS 5→6**	−5.6	4.2	−7.9	−10.8	−13.2	−7.7
$CH_2COH^+ \rightarrow CH_3^+ + CO$, TS_E	1.4	3.1	0.2	−3.6	−4.3	−21.6

[a] Geometries were optimized at the MP2/6-311++G(d,p) theory level. [b] ZPVE correction from MP2/6-311++G(d,p) frequencies. [c] At 700 K and 1.0 bar. Thermal corrections to Gibbs free energy and enthalpy were computed using the MP2/6-311++G(d,p) analytical frequencies, while electronic energies were calculated in an additive manner (see text for the details).

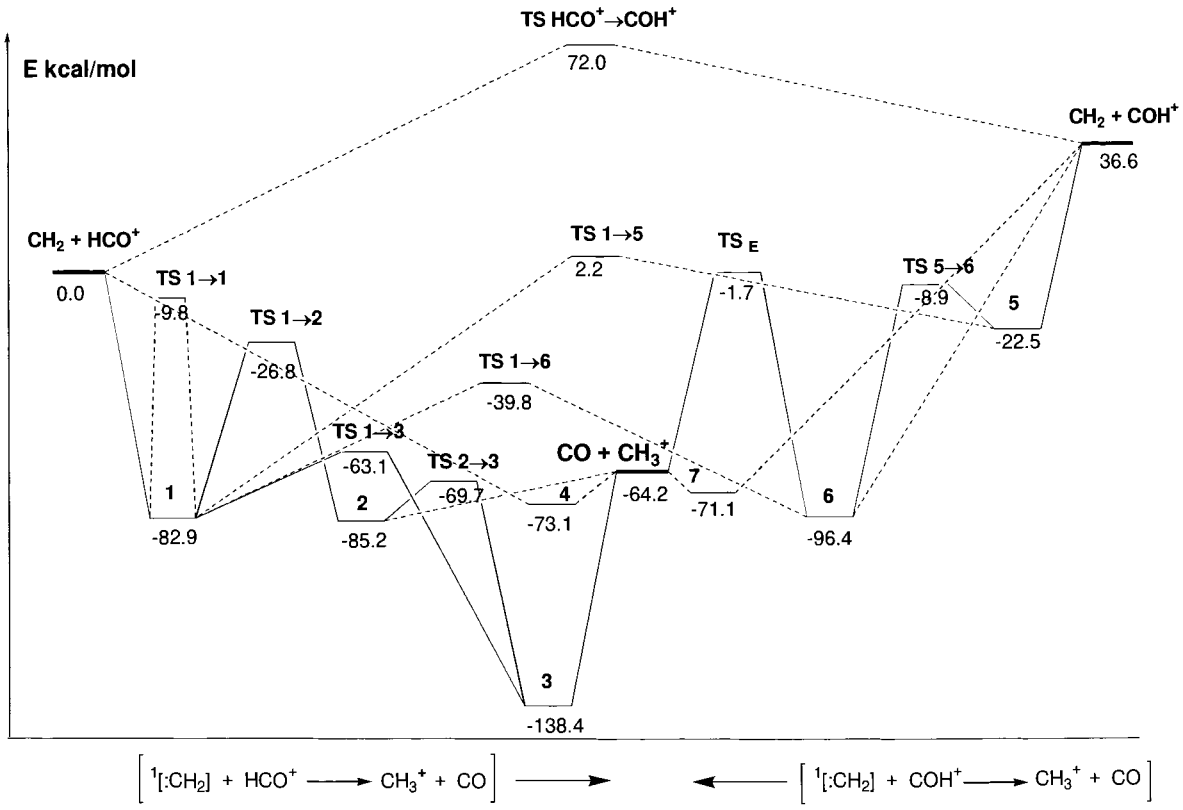

Figure 3. Energy profiles for the possible reaction channels corresponding to the reaction of formyl and isoformyl cations with $^1[:CH_2]$. Relative energies were calculated in an additive manner (see text for the details).

results are in close agreement with results from experiment and the additive theoretical procedure mentioned above.

$HCO^+ + {}^1[:CH_2] \rightarrow CH_3^+ + CO$. It is well-known that singlet carbenes readily insert into single C−H bonds of hydrocarbons and/or into O−H bonds, even without an activation barrier.[22] In the present process no TS was located for the direct insertion of $^1[:CH_2]$ into the H−C bond at the formyl cation. According to our calculations, the addition of $^1[:CH_2]$ to the π CO bond proceeds in a barrierless mode, rendering a cyclic intermediate **1** 82.9 kcal/mol more stable than reactants. In this

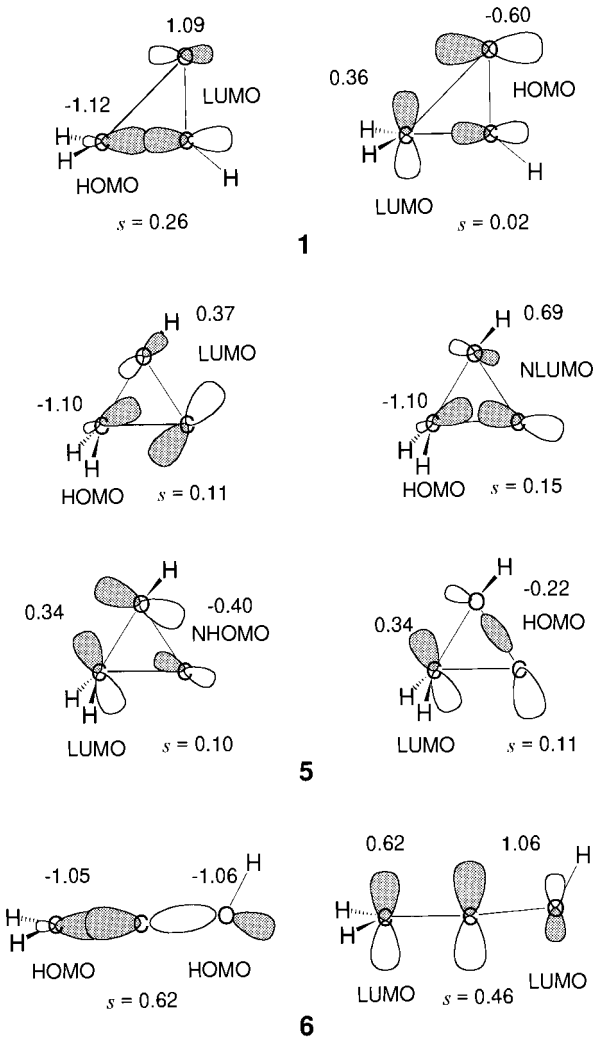

Figure 4. Sketch of the main orbital interactions between $^1[:CH_2]$ and the HCO^+ or COH^+ cations leading to the formation of the **1**, **5**, and **6** intermediates. Changes in the population of the frontier MOs and overlap (*s* in au) between the corresponding MOs are also indicated.

structure, the carbon atom of the singlet methylene is bound to both the carbon atom and the oxygen atom of the formyl moiety with respective bond lengths of 1.434 and 1.622 Å (see Figure 1). As the observed changes in the occupation numbers of the frontier MOs confirm, bonding in **1** occurs through HOMO($^1[:CH_2]$, sp^2) → LUMO(HCO^+, π) interaction (see Figure 4), rendering a net NPA charge transfer of 0.455 e. A TS, **TS1→1′**, was also located for the isomerization of **1** to its mirror image with an energy barrier of 73.1 kcal/mol. **TS1→1′** presents a quasi linear $CH_2-O-C-H$ arrangement in which the CH_2 fragment, situated along the molecular axis of the formyl moiety, is strongly bonded to the oxygen atom with a bond distance of 1.373 Å (see Figure 1).

The stable cyclic structure **1** may evolve through a TS for H shift from the carbon atom of the formyl fragment to the carbon atom of the methylene moiety (**TS1→2** in Figure 1), involving the simultaneous cleavage of the three-membered ring. **TS1→2** is 56.1 kcal/mol above **1** and presents a cyclic structure where the H_2C-O distance has decreased to 1.460 Å and the C−C distance has increased to 1.707 Å while the H atom of the formyl fragment is being transferred to the C atom of the CH_2 moiety. The corresponding IRC calculations show that **TS1→2** connects **1** with a linear intermediate CH_3OC^+, **2** in Figure 1, which is only 2.3 kcal/mol more stable than the cyclic intermediate **1**. **2** can be described as a Lewis donor−acceptor σ-complex formed by the methyl cation CH_3^+ interacting with the oxygen atom of a CO molecule ($H_3C\cdots OC$ distance is 1.594 Å). The binding energy is 21.0 kcal/mol, and the net NPA charge transfer from CO to CH_3^+ is 0.345 e. On the other hand, the cleavage of the cyclic intermediate **1** can also proceed through **TS1→3**, which is 19.8 kcal/mol less stable than **1**. At **TS1→3**, the cleavage of the weak H_2C-O bond at **1** has already taken place at the start of the H shift (see Figure 1). It is interesting to note that **TS1→3** resembles a TS for the insertion of $^1[:CH_2]$ into the C−H bond at the formyl cation. Nevertheless, the IRC reaction path confirms that **TS1→3** links the initial CH_2CHO^+ cyclic intermediate with an acylium ion intermediate (**3** in Figure 1). **3** is 138.4 kcal/mol more stable than the reactants and presents a linear arrangement with the CH_3 fragment located along the CO axis with a H_3C-CO distance of 1.441 Å. The calculated binding energy between the CH_3^+ and CO fragments at **3** amounts to 74.2 kcal/mol. Given that **3** is the most stable $C_2H_3O^+$ intermediate located on the MP2/6-311++G(d,p) PES, our calculations predict this structure as the $C_2H_3O^+$ ionic species implied in several reactions representative of a number of mechanisms going from CHO^+ to $C_3H_3^+$.[3,8]

2 and **3** are interconnected through a TS for the shift of CH_3^+ from C to O, **TS2→3**, which is 15.5 kcal/mol above **2**. The structure of **TS2→3** shown in Figure 1 can be described as a weak π-complex between the CH_3^+ cation and the CO molecule with a net NPA charge transfer of 0.171 e and a binding energy of 5.5 kcal/mol. Both **2** and **3** intermediates may dissociate into the products CO + CH_3^+, which are 64.2 kcal/mol more stable than the reactants, without passing through any saddle point (this was confirmed by means of reaction coordinate calculations varying CH_3^+-OC and CH_3^+-CO distances from **2** and **3**, respectively). However, a prediction of the most favored mechanistic route, that is, $^1[:CH_2] + HCO^+ \rightarrow$ **1** → **2** → CO + CH_3^+ vs $^1[:CH_2] + HCO^+ \rightarrow$ **1** → **3** → CO + CH_3^+, may require a detailed dynamical study on the PES.

Besides the ability of singlet methylene to add to double bonds, it is also a basic compound with a calculated proton affinity of 208.4 kcal/mol that can abstract a proton from acids such as HCO^+ where the corresponding base has a lower proton affinity (150 kcal/mol). Figure 1 presents an intermediate **4** that corresponds to a complex between CH_3^+ and CO with an equilibrium $CH\cdots C$ distance of 2.276 Å.[23] This structure is a minimum on the MP2/6-311++G(d,p) PES, 73.1 kcal/mol more stable than $^1[:CH_2] + HCO^+$ and 8.9 kcal/mol more stable than CH_3^+ + CO. A reaction coordinate following calculation shows that this intermediate is formed by proton transfer from HCO^+ to $^1[:CH_2]$ and can dissociate into products without any energy barrier.

$^1[:CH_2] + COH^+ \rightarrow CH_3^+ + CO$. The addition of $^1[:CH_2]$ to the CO bond at the isoformyl cation leads to a cyclic intermediate, **5**, 59.1 kcal/mol more stable than the initial fragments $^1[:CH_2] + COH^+$ (see Figures 2 and 3). In contrast with the structure of the cyclic intermediate **1**, all the bond distances in the three-membered ring of **5** are close to typical single bond values. Thus, in **5** the carbon atom of methylene is bonded to both the carbon and oxygen atoms of the isoformyl moiety, with bond lengths of 1.467 and 1.516 Å, respectively. However, the formation of **1** from $^1[:CH_2] + HCO^+$ is 23.8 kcal/mol more exoergic than the formation of **5** from $^1[:CH_2]$ + COH^+. This is consistent with a weaker orbital interaction in **5** than in **1** as observed in Figure 4. In effect, in **5** the $^1[:CH_2]$ → COH^+ charge transfer occurs through both HOMO−NLUMO

and HOMO−LUMO moderate overlaps whereas in **1** there is a larger HOMO−LUMO overlap. A 1,2-H-shift TS (**TS1→5** in Figure 2) for the isomerization of the CHO^+ moiety from isoformyl to formyl was located on the PES presenting a moderate energy barrier of 24.7 kcal/mol with respect to **5** and connecting this intermediate with **1**.

According to our calculations, the ring opening of the C−C−O triangle at **5** may proceed to a linear intermediate **6** through a low-energy barrier TS (**TS5→6** in Figure 2) in which the H_2C−O bond has elongated to 1.754 Å whereas the C−O bond length has diminished to 1.396 Å. This TS, **TS5→6,** has an activation energy of only 13.6 kcal/mol and therefore constitutes the most favorable route for the evolution of the **5** intermediate. **6** is a ketene molecule protonated at the oxygen atom and is 133.0 kcal/mol more stable than the methylene and the isoformyl cation. MP2/6-311++G(d,p) reaction coordinate calculations varying the C−C distance show that the formation of the **6** intermediate may also proceed through the direct attachment of $^1[:CH_2]$ to the C atom of COH^+. These calculations indicated that initially a π-approach between fragments is slightly more favorable than the corresponding linear σ-approach. Owing to the null HOMO−LUMO overlap between fragments in **6**, the resultant bonding is explained in terms of pseudoexcitation orbital interactions[24] controlled by HOMO−HOMO and/or LUMO−LUMO overlaps (see Figure 4) that render the HOMO of the supermolecule a linear combination of mainly the LUMOs of the fragments. **6** in turn may dissociate into the final products through a TS, $\mathbf{TS_E}$, for the 1,2-elimination of CH_3^+ with a high-energy barrier of 94.7 kcal/mol. This TS shows a nearly planar arrangement of the reactive bonds and has a transition vector very similar to that of the corresponding TS for the 1,2-H_2 elimination from protonated formaldehyde.[25] However, another competitive route for the evolution of **6** was located on the PES through a TS (**TS1→6** in Figure 2) with an energy barrier of 56.6 kcal/mol, 38.1 kcal/mol more stable than $\mathbf{TS_E}$. **TS1→6** presents the C−C−O atoms in a collinear arrangement, and its transition vector is dominated by the 1,2 H-shift between C and O atoms. The IRC reaction path confirms that this TS connects the linear intermediate **6** with the cyclic intermediate **1**.

Figure 2 shows a hydrogen-bonded complex **7** between CH_3^+ and CO, having an equilibrium CH···O distance of 2.178 Å. **7** is a minimum on the MP2/6-311++G(d,p) PES, 107.7 kcal/mol more stable than $^1[:CH_2] + COH^+$ and 6.9 kcal/mol more stable than $CH_3^+ + CO$. A reaction coordinate shows that this intermediate is formed by proton transfer from COH^+ to $^1[:CH_2]$ and can dissociate into products without any energy barrier.

It is interesting to note that **TS1→5** and **TS1→6** are TSs characterizing the rearrangement of the HCO^+ moiety into COH^+. Very recently, the results of the catalytic action of small neutral molecules attached to the H atom in the rearrangement of HCO^+ into COH^+ have been reported.[26] In general, the interaction with a neutral molecule leads to a significant lowering of the barrier for the rearrangement. Compared with the TS for the uncatalyzed isomerization between the formyl and isoformyl cations, the proton migration in $C_2H_3O^+$ structures takes place through considerably more favorable TSs than the direct process (see Figure 3).

Besides $C_2H_3O^+ \rightarrow CH_3^+ + CO$, other fragmentations could be considered to give $CH_2O + CH^+$ or $H_2C{=}C{=}O + H^+$. However, the products corresponding to these processes are 59.9 and 58.0 kcal/mol, respectively, less stable than the initial reactants $CH_2 + HCO^+$ and therefore do not constitute competitive alternatives (see Table 1).

Thermodynamic Analysis. To analyze the effect of temperature and entropy on the two processes presented above, we calculated the Gibbs free energies for all the structures implied at 700 K. Free energy profiles are qualitatively similar to the energy profiles in Figure 3 (see Table 1). All the intermediates and TSs involved in the $^1[:CH_2] + HCO^+ \rightarrow CO + CH_3^+$ reaction through the different mechanisms remain more stable than reactants. The acylium cation is considerably more stable than $CO + CH_3^+$ in free energy (49.9 kcal/mol), whereas the entropic contribution makes hydrogen complex **4** 17.4 kcal/mol less stable than the products. Concerning the $^1[:CH_2] + COH^+ \rightarrow CO + CH_3^+$ process, the free energy profiles also run parallel to the energy profiles in Figure 3 except for the entropic destabilization of intermediate **7** with respect to products (16.3 kcal/mol).

Conclusions

The energy profile displayed in Figure 3 describes various possible mechanisms for the reaction $^1[:CH_2] + CHO^+ \rightarrow CH_3^+ + CO$. The initial addition of $^1[:CH_2]$ to the formyl or isoformyl cations leads to the formation of both cyclic and linear $C_2H_3O^+$ intermediates. Most of the TSs for proton migration and/or ring opening of these intermediates are energetically more stable than reactants, so these intermediates may easily evolve to give open-chain CH_3CO^+ or CH_3^+···OC structures that in turn may readily dissociate to yield the final products. Two intermediates **4** and **7** corresponding to hydrogen-bonded complexes between CH_3^+ and CO were also located, characterizing a mechanism through a simple proton transfer from HCO^+ or COH^+ to singlet methylene. Finally, the great relative stability of the acylium cation **3** (about 138 kcal/mol below $^1[:CH_2] + CHO^+$) allows us to identify it as the $C_2H_3O^+$ species implied in several reactions representative of a number of mechanisms going from CHO^+ to $C_3H_3^+$.

Acknowledgment. The authors are grateful to the DGICYT (Spain) for financial support (PB94-1314-C03-01). N.D. also thanks the FICYT (Principado de Asturias) for a grant (FC-97-BECA-040). T.L.S. acknowledges the warm hospitality of all the members of the Department of Chemistry at the City University of New York.

Supporting Information Available: Table S1 containing total energies of all the structures studied in this work, Figure S1 representing Gibbs free energy profiles, and MP2/6-311++G(d,p) optimized geometries of reactanst, TSs, intermediates, and products (7 pages). Ordering information is given on any current masthead page.

References and Notes

(1) *Soot Formation in Combustion. Mechanisms and Models*; Bockhorn, H., Ed.; Springer-Verlag: Berlin, 1994.

(2) Haynes, B. S. In *Fossil Fuel Combustion*; Bartok, W., Sarofim, A. F., Eds.; Wiley-Interscience: New York, 1991.

(3) Calcote, H. F. *Combust. Flame* **1981**, *42*, 215.

(4) Olson, D. B.; Calcote, H. F. *Symp. (Int.) Combust., [Proc]* **1981**, *18*, 453.

(5) Calcote, H. F.; Olson, D. B.; Keil, D. G. *Energy Fuels* **1988**, *2*, 494.

(6) Eraslan, A. N.; Brown, R. C. *Combust. Flame* **1988**, *74*, 19.

(7) Michaud, P.; Delfau, J. L.; Barrasin, A. *Symp. (Int.) Combust., [Proc.]* **1981**, *18*, 443.

(8) (a) Miller, W. *J. Oxid. Combust. Rev*. **1969**, *3*, 97. (b) Goodongs, J. M.; Bohme, D. K.; Sugden, T. M. *16th International Symposium on Combustion*; Combustion Institute: Pittsburgh, PA, 1977; p 891.

(9) Frisch, M. J.; Trucks, G. W.; Schlegel, H. B.; Gill, P. M. W.; Johnson, B. G.; Robb, M. A.; Cheesman, J. R.; Keith, T. A.; Petersson, G. A.; Montgomery, J. A.; Raghavachari, K.; Al-Lahan, M. A.; Zakrzewski, V. G.; Ortiz, J. V.; Foresman, J. B.; Cioslowski, J.; Stefanov, B. B.; Nanayakkara, A.; Challacombe, M.; Peng, C. Y.; Ayala, P. Y.; Chen, W.; Wong, M. W.; Andres, J. L.; Replogle, E. S.; Gomperts, R.; Martin, R. L.; Fox, D. J.; Binkley, J. S.; Defrees, D. J.; Baker, J.; Stewart, J. P.; Head-Gordon, M.; Gonzalez, C.; Pople, J. A. *Gaussian 94*; Gaussian, Inc.: Pittsburgh, PA, 1995.

(10) Schlegel, H. B. *J. Comput. Chem.* **1982**, *3*, 211

(11) Hehre, W. J.; Radom, L.; Pople, J. A.; Schleyer, P. v. R. *Ab Initio Molecular Orbital Theory*; Wiley: New York, 1986.

(12) Bartlett, R. J. *J. Phys. Chem.* **1989**, *93*, 1697.

(13) McQuarrie, D. A. *Statistical Mechanics;* Harper & Row: New York, 1976.

(14) (a) Fukui, K. *Acc. Chem. Res.* **1981**, *14*, 363. (b) Gonzalez, C.; Schlegel, H. B. *J. Phys. Chem.* **1989**, *90*, 2154. (c) Gonzalez, C.; Schlegel, H. B. *J. Phys. Chem.* **1990**, *94*, 5523.

(15) Reed, A. E.; Weinstock, R. B.; Weinhold, F. *J Chem. Phys.* **1985**, *83*, 735.

(16) (a) Fujimoto, H.; Kato, S.; Yamabe, S.; Fukui, K. *J. Chem. Phys.* **1974**, *60*, 572. (b) Menéndez, M. I.; Sordo, J. A.; Sordo, T. L. *J. Phys. Chem.* **1992**, *96*, 1185.

(17) López, R.; Menéndez, M. I.; Suárez, D.; Sordo, T. L.; Sordo, J. A. *Comput. Phys. Commun.* **1993**, *76*, 235−249.

(18) Curtiss, L. A.; Redfem, P. C. Smith, B. J.; Radom, L. *J. Chem. Phys.* **1996**, *104*, 5148.

(19) Jensen, P.; Bunker, P. R. *J. Chem. Phys.* **1988**, *89*, 1327.

(20) (a) Bauslicher, C. W.; Taylor, P. R. *J. Chem. Phys.* **1986**, *85*, 6510. (b) Li, X.; Piecuch, P.; Paldus, J. *Chem. Phys. Lett.* **1994**, *224*, 267. (c) González, C.; Restrepo-Cossío, Márquez, M.; Wiberg, K. B. *J. Am. Chem. Soc.* **1996**, *118*, 5408

(21) (a) Freeman, C. G.; Knight, J. S.; Love, J. G.; McEwan, M. J. *Int. J. Mass Spectrom. Ion Processes* **1987**, *80*, 255. (b) Lias, S. G.; Bartmess, J. E.; Liebman, J. F.; Holmes, J. L.; Levin, R. D.; Mallard, W. G. *J. Phys. Chem. Ref. Data, Suppl.* **1988**, *17*. (c) Harland, P. W.; Kim, N. D.; Petrie, S. A. H. *Aust. J. Chem.* **1989**, *42*, 9.

(22) (a) Morrison, R. T.; Boyd, R. N. *Organic Chemistry*, 5th ed.; Allyn and Bacon: Boston, 1987. (b) Jones, M.; Moss, R. A. Carbenes. In *Reactive Intermediates*; Jones, M., Moss, R. A., Eds.; Wiley: New York, 1978. (c) Bach, R. D.; Su, M.; Aldabbagh, E. Andrés, J. L.; Schlegel, H. B. *J. Am. Chem. Soc.* **1993**, *115*, 10237.

(23) Uggerud, E. *J. Am. Chem. Soc.* **1994**, *116*, 6873−7869.

(24) (a) Fukui, K. *Theory of Orientation and Stereoselection*; Spinger Verlag: Berlin, 1975. (b) Suárez, D.; Sordo, J. A.; Sordo, T. L. *J. Phys. Chem.* **1996**, *101*, 13462.

(25) Suárez, D.; Sordo, T. L. *J. Phys. Chem. A* **1997**, *101*, 1561.

(26) (a) Chalk, A. J.; Radom, L. *J. Am. Chem. Soc.* **1997**, *119*, 7573. (b) Cunje, A.; Rodriguez, C. F.; Bohme, D. K.; Hopkinson, A. C. *J. Phys. Chem. A* **1998**, *102*, 478.